THE JOURNAL OF PHYSICAL CHEMISTRY B

ARTICLE

pubs.acs.org/JPCB

Electrochemically Induced Reversible and Irreversible Coupling of Triarylamines

Olena Yurchenko,[†,‡] David Freytag,[†,‡] Lisa zur Borg,[§] Rudolf Zentel,[§] Jürgen Heinze,[*,‡,⊥] and Sabine Ludwigs[*,†,‡,#]

[†]Freiburg Institute for Advanced Studies & Institut für Makromolekulare Chemie, Universität Freiburg, Albertstr. 19, 79104 Freiburg, Germany

[‡]Freiburger Materialforschungszentrum, Universität Freiburg, Stefan-Meier-Str. 21, 79104 Freiburg, Germany

[§]Fachbereich Chemie, Pharmazie und Geowissenschaften, Universität Mainz, Duesbergweg 10 −14, 55099 Mainz, Germany

[⊥]Institut für Physikalische Chemie I, Universität Freiburg, Albertstr. 21, 79104 Freiburg, Germany

Supporting Information

ABSTRACT: The electrochemical coupling and dimerization behavior of the low molecular compounds triphenylamine (**TPA**) and 9-phenylcarbazole (**PHC**) in comparison to tri-*p*-tolylamine (***p*-TTA**) with para-blocked methyl groups has been investigated in detail. In contrast to the unsubstituted radical cations of **TPA** and **PHC**, the radical cations of ***p*-TTA** are stable in the radical cation state and do not undergo any further coupling reactions. However, we found that the dicationic state of ***p*-TTA** does undergo two different competitive reaction pathways: (1) an irreversible intramolecular coupling reaction which leads to phenylcarbazole moieties and (2) a reversible intermolecular dimerization leading to charged σ-dimers. The σ-dimers become decomposed upon discharging at low potentials (E_{pc} = −0.97 V vs Fc/Fc$^+$) so that the starting monomer ***p*-TTA** is partially regenerated. In particular, the reversible dimerization reaction has not been described in literature so far. Polymeric systems containing para-methyl blocked triarylamines in the side chain exhibit similar coupling behavior upon electrochemical doping.

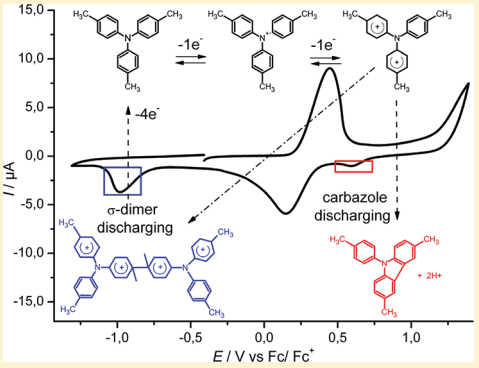

INTRODUCTION

Materials based on triphenylamine (**TPA**) and *N,N,N′,N′*-tetraphenylbenzidine (**TPB**) have found various applications as hole-transport materials in thin layer optoelectronic devices[2] such as xerography,[3] organic light emitting diodes (OLEDs),[4−6] organic solar cells,[7,8] and electrochromic devices[9] due to their easy oxidizability and hole transport mobilities up to 10^2 cm^2/V s.[10−13] Polymeric compounds, including derivatives containing **TPA** and **TPB** units in the side chain, have considered interest due to their easier processability and possibility to fabricate large-area devices by simple coating techniques. Charge transport in these systems takes place via radical cation species by a hopping mechanism.[10,14] The reversible formation of the radical cations is accordingly one of the most important requirements for these devices.

It is well-known that the one-electron oxidation of unsubstituted as well as partially substituted triphenylamines causes the generation of reactive radical cations, which typically undergo irreversible dimerization to **TPB**s as a result of oxidative coupling.[15−18] The dimerization occurs exclusively in the para position to the nitrogen centers, i.e., the sites with the highest spin electron density, and was observed also in side chain triarylamine polymers.[8,9,19] Substituents partially blocking the reactive para sites have a major influence on the coupling rate constant due to electronic effects.[15,17,20] Generated dimers can act as traps for positive charges within triphenylamine systems because of their higher-lying highest-occupied molecular orbital (HOMO) in relation to the vacuum level.[21,22] In the literature one can often find the statement that the dimerization reaction can be prevented either by blocking the reactive para sites or by stabilizing the radical cations with electron donating substituents such as methyl, methoxy, and amino groups.[8,17,23,24] Our experiments of *para*-methyl-substituted **TPA** however demonstrated that coupling is possible. Details will be presented below.

The dimerization reaction of **TPA** radical cations is interpreted in analogy to the initial oxidative coupling of conjugated monomers such as thiophene, pyrrole, and aniline. In this case, oxidation leads to highly reactive radical cations which rapidly couple to charged σ-dimers as intermediate species.[25,26] After proton elimination neutral dimers are formed, which then may undergo further oxidation and coupling steps leading to extended conjugated systems, i.e., oligomers and polymers. The driving force for these radical cation/radical cation coupling reactions is a high spin density at characteristical positions in the molecules.

Received: August 22, 2011
Revised: November 14, 2011
Published: December 12, 2011

The stability of π-conjugated radical cations can be increased by extension of the conjugated system[26−28] and/or the substitution with electron donating groups at appropriate positions[29,30] as well as by the protection of reactive sites[31,32] or insertion of sterically demanding structural units.[33]

Intermolecular interactions between relatively stable radical ions can result in the reversible formation of spinless dimers. The reversible self-association or coupling of π-conjugated radical ions has been observed by numerous research groups, e.g. for radical anions of 9-fluoro-10-cyanoanthracene (**FCA**$^{\bullet-}$) and 9-cyanoanthracene as well as for radical cations of octamethylbiphenylene (**OMB**$^{\bullet+}$) and alkylated oligothiophenes.[34−40] The formation of dimers in these reports was proven by the concentration- and temperature-dependence of cyclic voltammetric (CV) measurements, electron paramagnetic resonance (EPR), and UV/vis spectra. In the case of radical anions, the formation of σ-dimers has been widely accepted, whereas π or σ-dimerization are discussed in the case of radical cations. Interestingly, the X-ray analysis of crystalline radical cation salts very often exhibited sandwich stacked units with relative long bonding indicating the $\pi-\pi$ interaction, e.g., in the case of 3′,4′-dibutyl-5,5″-diphenyl-2,2′:5′,2″-terthiophene.[41]

Concerning the reversible formation of cationic σ-dimers, Heinze et al. were one of the first to report on this matter.[1,42,43] In contrast to the data of π-dimerization which are exclusively based on spectroscopic findings, evidence of σ-dimerization has been obtained from additional voltammetric and thermodynamic findings. Thus, voltammetric measurements on alkylated bithiophenes and diphenylpolyenes show at higher scan rates an additional cathodic wave at a potential negative to the original signal of the radical cation reduction, indicating a reversible follow-up reaction.[1,25,30,43,44] It has been shown that the formation of charged σ-dimers can take place even in spite of sterical hindrance of reactive positions.[32,43,45,46] The evaluation of thermodynamic quantities such as reaction enthalpies has revealed that their values lie between −60 and −90 kJ mol^{-1}.[1,37,43] In view of the continued Coulombic repulsion this indicates a considerable bonding enthalpy excluding a weak π-interaction.[34]

In this manuscript, we study the coupling behavior of unsubstituted **TPA**, methyl-substituted tri-*p*-tolylamine (***p*-TTA**) as well as polymeric systems based on methyl substituted triphenylamine directly attached to a polymer backbone termed as **PoTTA**, upon electrochemical oxidation by in situ spectroelectrochemistry. Our experiments identify two types of follow-up reactions, electrochemically induced reversible and irreversible coupling.

The in situ spectroelectrochemistry measurements are performed under thin-layer conditions. Under these conditions the complete electrolysis of the investigated compounds is ensured (within a few seconds) allowing a direct and easy spectroscopic identification of followup products.

EXPERIMENTAL SECTION

The spectroelectrochemical experiments were performed in a thin-layer cell constructed by Geskes with a standard three-electrode arrangement in the reflection mode using a polished platinum disk (d = 4 mm) sealed in soft glass as a mirror type working electrode (WE).[47] The WE was connected with a micrometer screw allowing the varying of the cell thickness by adjustment of the distance between cell bottom and WE. Additionally, the cell was equipped with an internal cooling shell. A platinum wire, wrapped around the glass of the WE served as the counter electrode, and a silver wire as the pseudoreference electrode (RE). For potential calibration, the redox couple ferrocene/ferrocenium [$E_{1/2}$(Fc/Fc$^+$ vs Ag) ≈ 0.42 V] was used as internal standard. The voltammetric experiments were carried out under argon atmosphere at scan rates of 20 mV s^{-1} in dichloromethane/0.1 M tetrabutylammonium hexafluorophosphate ($TBAPF_6$) solution under finite diffusion conditions with a distance between cell bottom and WE of 20−80 μm. The concentration of the samples ranged from 0.7 mM to 2 mM. The CVs were measured with an AutoLab Potentiostat-Galvanostat PGSTAT101 or with a JAISSLE Potentiostat-Galvanostat IMP 88 PC controlled by an EG&G PARC Model 175 Universal Programmer. In situ UV/vis spectra were recorded with a Zeiss modular spectrometer system with MCS 500-components (Lampenkassette CLH 500, Spektrometerkassette MCS 521 Vis, fiber optic). The absorption of the sample solution during the electrochemical charging/discharging was calculated from the difference of the light emitted and reflected from the working electrode.

Cyclic voltammetry experiments under semi infinite diffusion conditions (under normal conditions) were carried out under argon atmosphere in a cell with platinum disk (d = 1 mm) as WE, a platinum wire as counter electrode, and Ag/AgCl wire as a RE [$E_{1/2}$(Fc/Fc$^+$ vs AgCl) ≈ 0.37 V] in dichloromethane/0.1 M $TBAPF_6$ solution at different scan rates. The concentration of ***p*TTA** in the electrolyte was 1 mM.

Dichloromethane (hypergrade) was purchased from Sigma-Aldrich and purified by distillation over CaH_2 under argon atmosphere prior to use. $TBAPF_6$ (puriss.) was purchased from Fluka and used as received. Triphenylamine (97%) purchased from Merck, *N,N,N′,N′*-tetrakis(phenyl)benzidine (98%) purchased from ABCR, 9-phenylcarbazole (purity >99%), and tri-(s)-*p*-tolylamine (97%) purchased from Sigma-Aldrich were used as received.

Para-methylated vinyltriphenylamine monomer was synthesized according to the literature.[5] For polymerization the monomer was dissolved in THF; then the THF was evaporated, and the resulting melt was polymerized at 45 °C. The obtained polymer **PoTTA** had a number molecular weight (M_n) of 170 000 g/mol as determined by gel permeation chromatography (compared to polystyrene samples) (data not shown).

RESULTS AND DISCUSSION

Irreversible Dimerization: Unsubstituted Triarylamine and 9-Phenylcarbazole. In Figure 1 the oxidation of unsubstituted triphenylamine (**TPA**) (a) and 9-phenylcarbazole (**PHC**) (b) which is structurally similar to **TPA** and follows an identical reaction path is shown under the conditions of a thin layer cell. The corresponding CVs exhibit during the first forward scan one high oxidation wave which corresponds to the oxidation of monomeric species to radical cations and subsequent oxidations of follow-up products. As already described in the literature, the follow-up reaction involves the formation of neutral dimers and their oxidation to radical cations and dications.[15,48,49] The reduction of the dications of the dimeric *N,N,N′,N′*-tetrakis(phenyl)benzidine (**TPB**) can be seen in the reverse scan (Figure 1a), in which two separate reduction waves indicate the formation of the monocation and then of the neutral dimer. This is consistent with the CV data of the dimeric species **TPB** (compare Figure 1a, inset). In the case of the **PHC** oxidation, which leads to the generation of *N,N′*-diphenyl-3,3′-bicarbazyl (**DPBC**), the reduction waves of the dimer are relatively small due to the partial

dx.doi.org/10.1021/jp208076z |*J. Phys. Chem. B* 2012, 116, 30–39

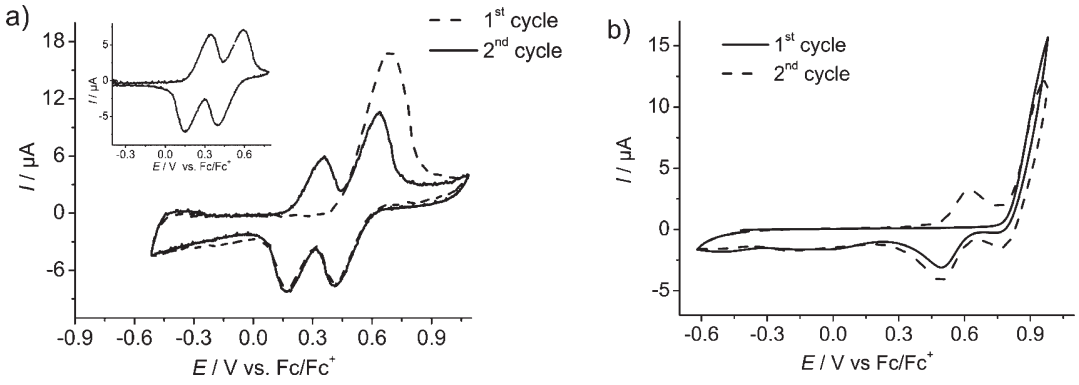

Figure 1. (a) CV of **TPA** oxidation with CV of **TPB** (1 mM) oxidation as inset and (b) CV of **PHC** (0.7 mM) oxidation at room temperature in the thin-layer cell (0.1 M $TBAPF_6/CH_2Cl_2$ solutions, ν = 20 mV s^{-1}). The corresponding UV/vis spectra are shown in Figures S1−S3 of Supporting Information. The detailed mechanism of the oxidation of **TPA** and **PHC** is shown in Scheme 1.

Scheme 1. Dimerization Mechanism of TPA (a) to TPB and PHC (b) to DPBC upon Oxidation

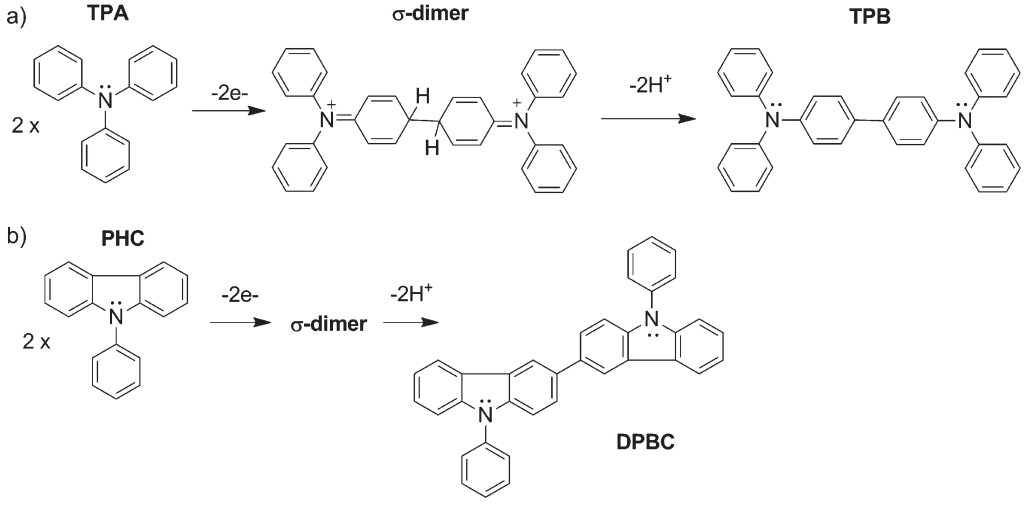

oxidation of the starting monomer and the decrease of the concentration of the dimer.[49] Therefore, the dication reduction of **DPBC** can be detected only in the reverse scan of the second cycle.

After the oxidation to the corresponding radical cations, both species couple under generation of covalent bonds to dicationic σ-dimers. Subsequently, two protons per bond are rapidly eliminated and the neutral dimers **TPB** and **DPBC** are formed, respectively (Scheme 1). The proton elimination takes place on the time scale of the experiment.

The generated dimers are more easily oxidized than the corresponding monomers and undergo at the applied potentials in the range of 0.7 to 0.9 V oxidation to their radical cations and then to dications. At high concentrations additional electropolymerization reactions have been observed.[49,50]

The UV/vis spectra recorded in situ during the oxidation of **TPA**, **PHC**, and **TPB** (see Figures S1−S3 of Supporting Information and the discussion there) confirm the dimerization mechanism. The spectroscopic monitoring of the oxidation processes points out that the coupling reaction of radical cations and the following proton release occur relatively fast. In the case of **TPA**, the absorption of monomer radical cation can be detected at the beginning of the oxidation, whereas no absorption of the radical cations has been registered during oxidation of **PHC**. This observation coincides with the data obtained by Ambrose,[48] who reported much higher reactivity of **PHC** radical cations due to the planar geometry of the carbazole moiety resulting in higher spin densities at the reactive sites and accordingly enhanced coupling rate (10^6 mol^1 s^1)[49] relative to the corresponding **TPA** radical cations (10^3 mol^1 s^1). The lifetime of the **PHC** radical cations is in the lower millisecond range and cannot be detected with our measurement setup. The absorption of the σ-dimers was not seen either, probably due to the high reactivity and short-lifetime of these species. According to Nelson et al.,[15] the coupling reaction of two radical cations seems to be a rate-determining step for triarylamine systems, whereas the proton loss should be relatively fast (in all investigated 4-substituted triphenylaminium ions). The rate of proton elimination depends on the presence of bases. Thus, traces of water in acetonitrile increase the rate of the elimination reaction.[26]

The absorption maxima obtained during oxidation of **TPA**, **TPB**, and **PHC** are summarized in Table 1.

Trimethylsubstituted Triphenylamine: p-TTA. Similarly to substituted oligothiophenes,[28,43] where the blocking of reactive α-positions increases the stability of their radical cations, the substitution of all hydrogen atoms at the *p*-phenyl position of

dx.doi.org/10.1021/jp208076z |J. Phys. Chem. B 2012, 116, 30–39

Table 1. Characteristic Absorption Bands Observed with in Situ Spectroelectrochemistry Measurements with Assignment to Respective Redox Species

	λ_{max} [nm]		
species	neutral	radical cation	dication
TPA before conversion	302	340, 562, 658	
TPA after conversion (identical to **TPB**)	352	484	722, 450
TPB	352	484	722, 450
PHC before conversion	328, 341	not determined	
PHC after conversion (corresponds to **DPBC**)		430, broad band at 1000	700, 757

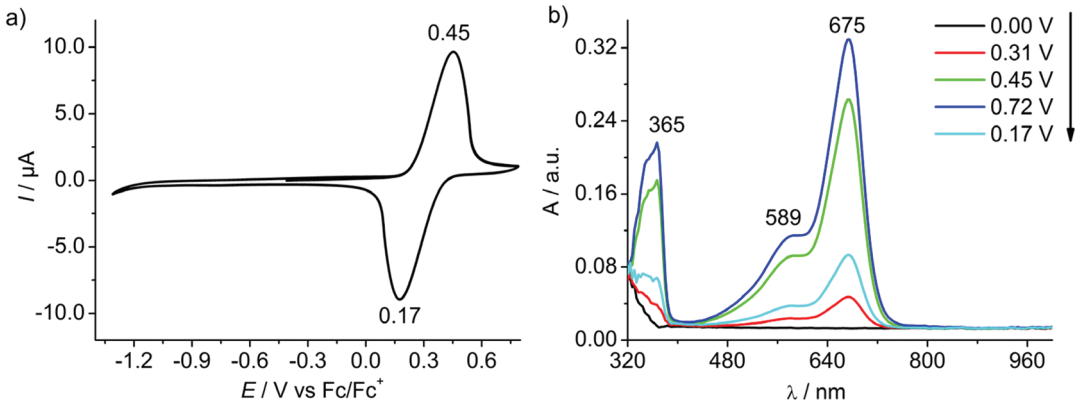

Figure 2. First cycles of the oxidation of ***p*-TTA** to the radical cation ***p*-TTA$^{\bullet+}$** (a) and corresponding UV/vis absorption spectra (b) at different potentials in the first cycle; 0.1 M $TBAPF_6/CH_2Cl_2$ solution, 2 mM, 20 mV s^{-1}, −45 °C.

triphenylamines with methyl groups considerably stabilizes their radical cations.[17,23,24]

The radical cations of trimethylsubstituted triphenylamine, ***p*-TTA**, are considered to be extremely stable species. The EPR spectra of in situ generated radical cations show practically no intensity decrease with time.[17] The CV experiments (not shown) as well as spectroelectrochemistry experiments at various conditions manifest the high stability of ***p*-TTA** radical cations. At first we discuss results obtained for low-temperature experiments. Figure 2a shows the first two cycles of an oxidation of ***p*-TTA** in a potential range up to 0.8 V. The measurements were carried out in a spectroelectrochemical cell in CH_2Cl_2 at −45 °C. One redox signal at $E_{1/2}$ = 0.31 V with a peak current ratio I_{pc}/I_{pa} of about 0.99 indicates the chemical reversibility of the oxidation and the stability of the radical cation ***p*-TTA$^{\bullet+}$**.

Compared to the CV of **TPA**, the oxidation potential of ***p*-TTA** is shifted to more negative potentials which can be attributed to the electron-donating effect of the methyl groups.

The corresponding absorption spectra (Figure 2b) reveal the development of three radical cation bands of ***p*-TTA$^{\bullet+}$** with maxima of 365, 589, and 675 nm. This absorption pattern is characteristic for the formation of radical cations of triarylamines.[51]

Further increase of the potential up to 1.4 V shows the next redox step of the ***p*-TTA** oxidation at about 1.2 V leading to its dication (Figure 3a). The oxidation wave has been measured only partially, because impurities such as water in the solvent may generate undesirable side reactions. Interestingly, there is no corresponding reduction wave in the reverse scan, pointing toward an irreversible process involving chemical follow-up reactions. Consequently, under thin-layer conditions the peak current ratio I_{pc}/I_{pa} for the first redox step ***p*-TTA/*p*-TTA$^{\bullet+}$** is also significantly smaller than 1.

Waves of the follow-up products can be seen in the reverse scan and subsequent cycles (Figure 3a). Redox waves with peaks at E_{pa} = 0.72 V and E_{pc} = 0.58 V ($E_{1/2}$ = 0.65 V) give evidence for a chemically reversible redox process. In addition to this redox pair, a pronounced cathodic wave is observed at −0.97 V.

As the wave at −0.97 V is always significantly larger than the signal of the redox pair at $E_{1/2}$ = 0.65 V one should conclude that competing reactions after the formation of ***p*-TTA^{2+}** occur. Surprisingly, the current heights of the redox waves at $E_{1/2}$ = 0.30 V (***p*-TTA/*p*-TTA$^{\bullet+}$**) and E_{λ_1} = 1.40 V (***p*-TTA$^{\bullet+}$/ *p*-TTA^{2+}**) depend on the lower switching potentials E_{λ_2} during voltammetric multisweep experiments (Figures 3a and 4a).

In the case that the lower switching potential E_{λ_2} lies at −0.4 V (Figure 4a), the heights of the redox waves of the ***p*-TTA** oxidation up to the dication strongly diminish during the second and third cycle, whereas the heights are constant or only slightly decrease during all cycles using a lower switching potential of −1.3 V (Figure 3a). This gives evidence that in the latter case the starting system, i.e., the neutral ***p*-TTA** is partially regenerated after the reductive decay of a species at −0.97 V. It should be noted that in thin-layer cells all the starting species are consumed during slow voltammetric sweeps. They are regenerated only in the case of reversible follow-up reactions.

Findings from the CVs suggest that follow-up processes at the level of the dication involve two competing reaction sequences with different coupling steps.

The formation of new species upon increase of the potential up to 1.4 V is further supported by the UV/vis spectra (parts b and c of Figure 3). For clarity reasons we also show the absorption bands at 675 (***p*-TTA$^{\bullet+}$**), 392, and 796 nm as function of the changing potentials during CV measurements (Figure 3d).

dx.doi.org/10.1021/jp208076z |*J. Phys. Chem. B* 2012, 116, 30–39

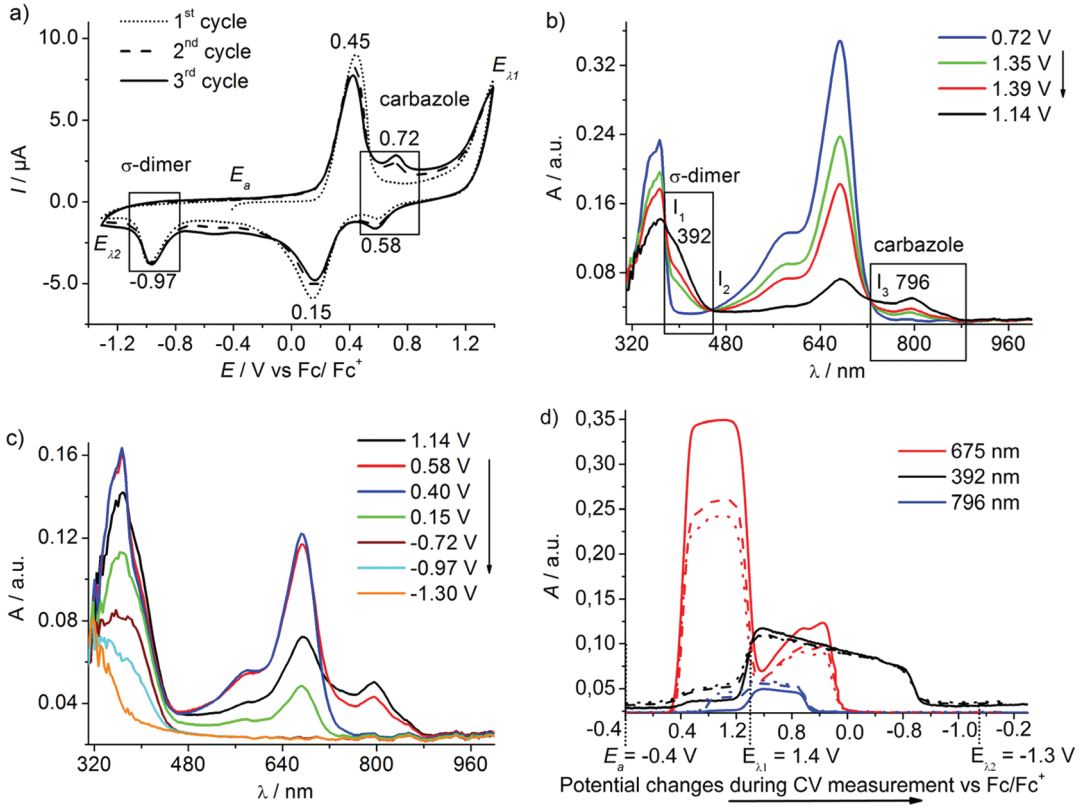

Figure 3. (a) CV of ***p*TTA** oxidation from −1.3 V up to 1.4 V, 2 mM, CH_2Cl_2/0.1 M $TBAPF_6$, 20 mV s^{-1}, −45 °C. UV/vis spectra at different potentials recorded in the first cycle during (b) oxidation at potentials above 0.72 V and (c) reduction between 1.14 and −1.30 V. (d) Evolution of the characteristic absorption bands during the oxidation of ***p*-TTA** in the first (solid line), second (dashed line), and third (dotted line) voltammetric cycle between E_a = −0.4 V and E_{λ_1} = 1.4 V (forward scan) and E_{λ_1} = 1.4 V and E_{λ_2} = −1.3 V (backward scan), respectively.

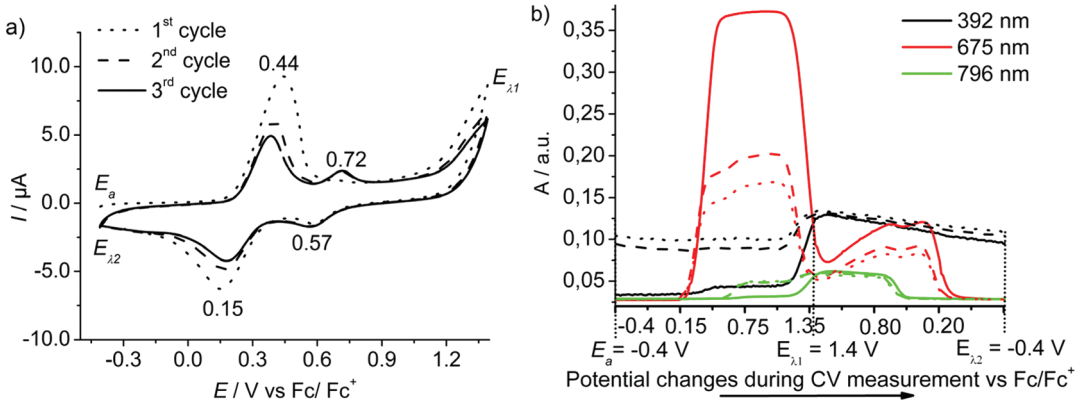

Figure 4. (a) CV of ***p*-TTA** oxidation recorded in the potential range from −0.4 to 1.4 V, 2 mM, CH_2Cl_2/0.1 M $TBAPF_6$, 20 mV s^{-1}, −45 °C. (b) Evolution of the characteristic absorption bands during the oxidation of ***p*-TTA** in the first (solid line), second (dashed line), and third (dotted line) voltammetric cycle between E_a = −0.4 V and E_{λ_1} = 1.4 V (forward scan) and E_{λ_1} = 1.4 V and E_{λ_2} = −0.4 V (backward scan), respectively.

While the radical cation signals of ***p*-TTA$^{\bullet+}$** decrease at potentials higher than 1.2 V, the appearance of two new bands around 392 nm and at 796 nm is observed (parts b and d of Figure 3). In this potential range one would expect formation of the dicationic form ***p*-TTA^{2+}**. However measurements of tri-*p*-anisylamine by Lambert et al.[51] show that the absorption signal of the dication appears in the spectral region between 400 and 600 nm, suggesting products of follow-up reactions in our case.

Figure 3c shows characteristic absorption spectra on the reverse scan of the first cycle. From 1.4 to 0.8 V a slight decrease of the band at 796 nm accompanied by rise of the radical cation bands ***p*-TTA$^{\bullet+}$** is observed. In the potential range between 0.8 to 0.4 V (see spectra at 0.58 and 0.40 V)—which corresponds to the cathodic wave at E_{pc} = 0.58 V—the absorption at 796 nm disappears, whereas the band around 392 nm is still clearly visible. Only at ∼−1.2 V does the band at 392 nm disappear as well. In the CV this corresponds to the cathodic wave at −0.97 V. This again

dx.doi.org/10.1021/jp208076z |*J. Phys. Chem. B* 2012, 116, 30–39

Scheme 2. Formation of Methylsubstituted Phenylcarbazole MMPC from *p*-TTA by Electrochemical Oxidation

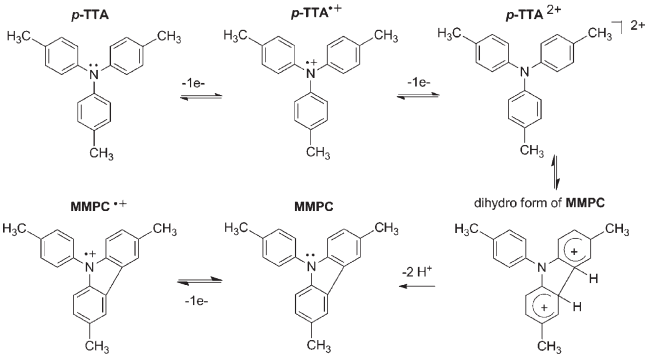

suggests the formation of two different follow-up species during oxidation of ***p*-TTA**$^{\bullet+}$ to its dication.

In the following the two competing reaction pathways will be further discussed.

(a). Irreversible Coupling Reaction (Intramolecular). According to Nelson et al., oxidation of tri-*p*-substituted triphenylamines and analogous derivatives leads to reactive dicationic species.[52] They investigated a number of substituted **TPA**s and discussed follow-up reactions upon oxidation to the dicationic state. In the case of ***p*-TTA**, the CVs exhibited the formation of a new redox pair, the oxidation of which is positive to that of the primary amine system. The comparison of spectroscopic and electrochemical data with those of a chemically synthesized carbazole unambiguously confirmed the formation of carbazole during the generation of the dicationic state. The conversion of aromatic amines to carbazoles via intramolecular cyclization was also observed for other triarylamine compounds, such as substituted tetrabenzidines. Dunsch et al. reported the transformation of *N,N,N′,N′*-tetrakis(4-methoxyphenyl)-benzidine into a new product with carbazole moieties after the oxidation to its tetracation.[53]

In our case, the reversible redox wave at $E_{1/2}$ = 0.62 V can be attributed to the oxidation of 3,6-dimethyl-*N*-(*p*-methylphenyl)carbazole (**MMPC**) after its generation in the potential range between 1.2 and 1.4 V. Scheme 2 represents the reaction pathway by intramolecular cyclization accompanied by irreversible elimination of two protons from the dihydro form.

The half wave potential is in good agreement with data reported in literature for **MMPC** with $E_{1/2}$ = 1.08 V vs SCE (0.68 V vs Fc^+/Fc).[48] The shift of $E_{1/2}$ to more positive values of **MMPC** compared to ***p*-TTA** can be attributed to the free electron pair at the nitrogen in the aromatic system of the carbazole unit.[54]

The absorption band at 796 nm is assigned to the radical cation **MMPC**$^{\bullet+}$ appearing after oxidation of **MMPC** and is in accordance with the literature (λ_{max} of radical cation =787 nm).[48] The formation of **MMPC** is an irreversible reaction and therefore consumes original ***p*-TTA**-molecules. An important point is that after the intramolecular coupling step two protons are eliminated which lower the local pH in front of the electrode. The high proton concentration may diminish the elimination rate of protons and protonate the remaining triarylamine base, facilitating competing reactions.

In the second scan during charging the appearance of the radical cation bands ***p*-TTA**$^{\bullet+}$ are observed first followed by the emergence of absorption bands characteristic for the carbazole radical cation **MMPC**$^{\bullet+}$ (see the evolution of the band at 675 and 796 nm in Figure 3d and also the spectra in Figure S4 of Supporting Information). Subsequent cycles always show the reversible oxidation of ***p*-TTA** and **MMPC**.

Scheme 3. *σ*-Dimer Formation on the Dicationic State of *p*-TTA

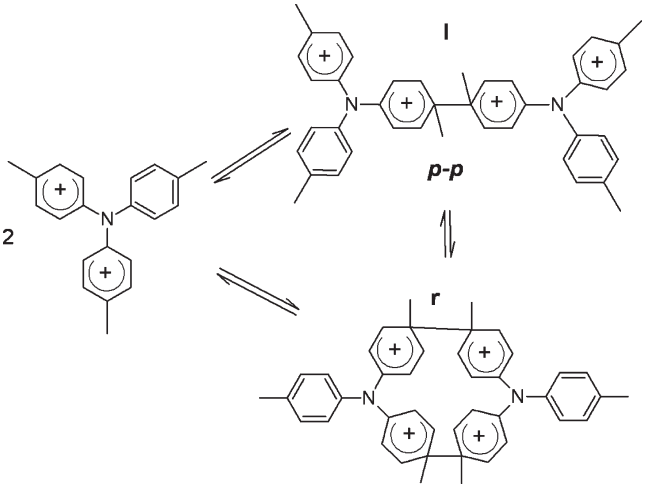

The absence of a dication absorption suggests that the follow-up reactions occur rapidly ($k > 10\ s^{-1}$), which is also in agreement with the results of Nelson et al. who reported extremely high cyclization rates.[52]

(b). Reversible Coupling (Intermolecular). In addition to the irreversible reaction, we have found a second mechanism not described in the literature yet.

The development of the new cathodic peak at −0.97 V (Figure 3a) can be correlated with the existence of reversibly generated charged *σ*-dimers according to data reported by Rasche and Heinze.[46] They observed a similar electrochemical behavior for *N,N*-dimethyl-*p*-toluidine with the only difference that *σ*-dimer formation occurred after oxidation to the radical cation. The one electron oxidation of toluidine led to a dimerization reaction of radical cations under formation of dicationic *σ*-dimers, which were stable in the charged state. After discharging at highly negative potentials, the dimers decayed into the neutral starting species. This was a strong indication that *σ*-dimers are very stable compared to the corresponding monomeric cation.

In our example, the cathodic wave at −0.97 V can also be explained by the reductive decay of *σ*-dimers regenerating the starting species. The main difference between ***p*-TTA** and toluidine is that here the dimerization reaction takes place at the level of the dicationic species. The formation of *σ*-dimers from a dicationic state has not been reported in the literature so far. However, the fact that intramolecular coupling to a carbazole unit occurs also from dications, suggests an intermolecular coupling as a competing process. We believe that the higher reactivity of ***p*-TTA** dications (compared to that of radical cations) allows the intermolecular coupling reaction in spite of Coulombic repulsion.

In principle, it is conceivable that these *σ*-dimers are formed from the newly generated carbazole. In this case, no voltammetric signal of carbazole should be seen during subsequent scans between −0.3 V and +1.4 V. In fact, reduction and oxidation waves of the monomeric radical cation of carbazole becomes visible within all cycles after the generation of ***p*-TTA**$^{2+}$ dication excluding any *σ*-dimerization of carbazole species.

The intermolecular coupling reaction of dicationic species ***p*-TTA**$^{2+}$ may produce a number of different species. Scheme 3 shows a

dx.doi.org/10.1021/jp208076z |*J. Phys. Chem. B* 2012, 116, 30–39

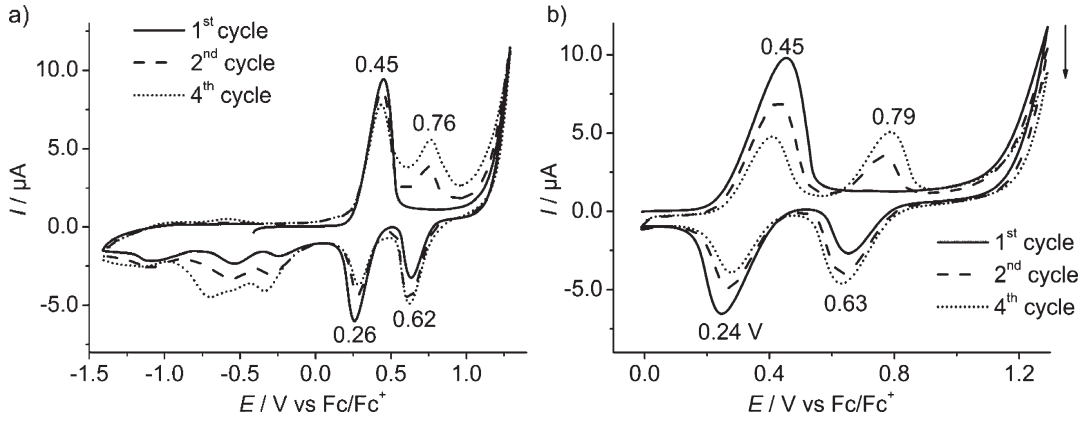

Figure 5. CVs of ***p*TTA** oxidation recorded in spectroelectrochemical thin layer cell in the potential range (a) from −1.4 to 1.3 V and (b) from 0 to 1.4 V; 2 mM, 20 mV s^{-1}, 20 °C.

linear tetracationic dimer (**l**) with random charge distribution. Assuming that the highest spin density is in para position to nitrogen, the *p*-*p* coupling product seems to be the most probable. Irreversible elimination of protons can be ruled out in this case. Other linear coupling products are given in Scheme S1 of Supporting Information. For those products the proton release leading to irreversible formation of new species cannot be excluded.

A ring structure (**r**) as given in Scheme 3 could also explain a tetracationic species. Here the discharge of the cyclic σ-dimers should occur within one reduction step due to the symmetrical charge distribution which is also consistent with the CV.

The UV/vis spectra support the interpretation of a σ-dimer formation in the dicationic state of ***p*-TTA** but cannot prove the nature of the product. The position of the band at 392 nm is similar to those of other σ-dimers that have been formed by the intermolecular coupling of conjugated radical cations.[45,55] Moreover, the band develops at the same time as the second oxidation of ***p*-TTA** takes place and disappears simultaneously with the cathodic discharging of the follow-up product at −0.97 V (Figure 3d).

The question remains why the intermolecular coupling occurs on the dicationic stage. One could assume that the reaction takes place at the radical cationic stage but with a much lower rate constant of dimerization. We could not detect this (Figure 2a). In agreement with the literature, the dicationic species ***p*-TTA**$^{2+}$ is more reactive than radical cations because of higher charge density.[48] The formation of carbazole from the dicationic state ***p*-TTA**$^{2+}$ underlines the reactivity of this charged species compared to the radical cation of ***p*-TTA** originating from a higher spin electron density in the phenyl rings.

For proving the reversible nature of the σ-dimer formation, CVs were also recorded in the potential range excluding the reduction of formed σ-dimers, i.e., CVs were taken between −0.4 and 1.4 V (Figure 4a). In this case, the reductive cleavage of the σ-bond of the dimer should be prevented.

In contrast to CVs including the cathodic wave at −0.97 V (compare Figure 3a), the CV in Figure 4a exhibits a strong and continuous decrease of the current of the first redox wave corresponding to the ***p*-TTA** oxidation with each cycle; wheares the redox peaks of **MMPC** do not increase at the same time. Similarly the intensity of the second oxidation wave which is related to the partial oxidation of the ***p*-TTA**$^{\bullet+}$ to the dication decreases continuously. This indicates a lowering in the concentration of ***p*-TTA** because of partial consumption by "irreversible" formation of σ-dimers. Both experiments provide

Chart 1. Structures of Investigated Side-Chain TPA Polymers

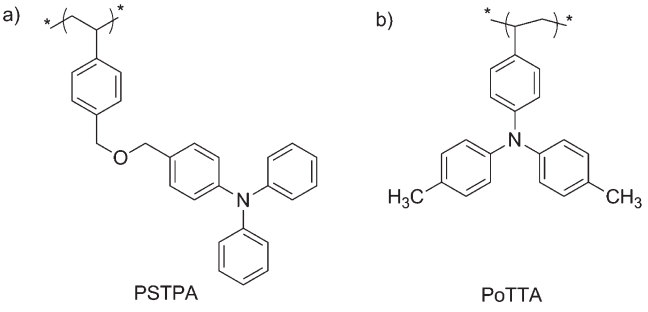

further evidence that the reduction of the σ-dimers leads to the primary educt ***p*-TTA**, when scanning to potentials below −1.2 V. The UV/vis spectroscopy measurements (Figure 4b) support the CV data.

Furthermore CV experiments under normal (semi-infinite) conditions using different scan rates were carried out. CVs together with a discussion are given in the Supporting Information (see Figure S5). These experiments compared to those under thin layer conditions did not provide any further information.

Experiments at Room Temperature. For comparison reasons and to study the coupling reactions further the in situ spectroelectrochemistry experiments were also performed at room temperature.

In Figure 5, two CVs recorded at 25 °C in different potential ranges, with (a) and without (b) reduction of σ-dimers, are presented. The left as well as the right CV show several distinctive redox waves with E_{pa} at 0.76 or 0.79 V and E_{pc} at 0.62 or 0.63 V, respectively. They result from the electrochemical oxidation and reduction of carbazole that has been formed as a follow-up product after the oxidation of the ***p*-TTA** monocation to its dication at 1.4 V. The higher peak currents compared to CVs obtained at low temperatures (Figure 3a) reveal a relatively high carbazole concentration. In Figure 5a, several small cathodic peaks at negative potentials are visible, which can be related to different coupling products as well as to products of solvent decomposition.

The absorption spectrum of the radical cation and the spectrum recorded after oxidation to the dication are available in Figure S6 of Supporting Information.

dx.doi.org/10.1021/jp208076z |*J. Phys. Chem. B* 2012, 116, 30–39

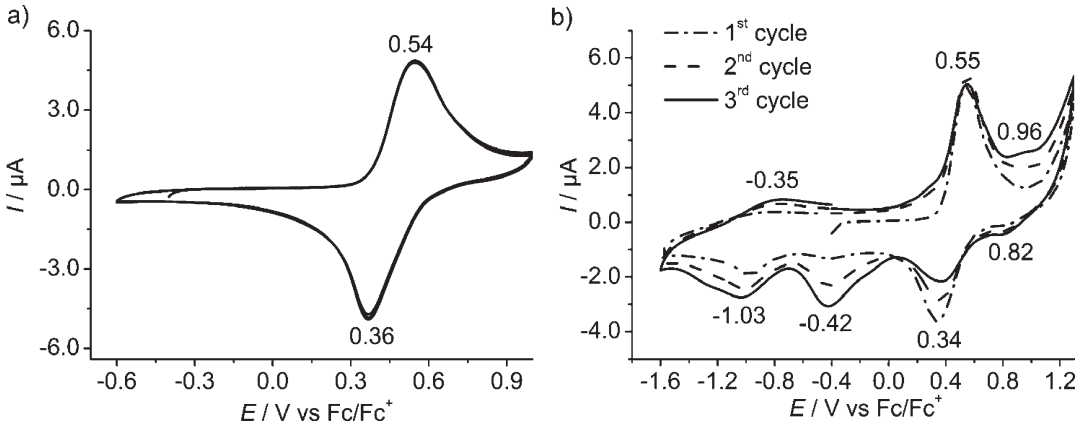

Figure 6. CV of PoTTA oxidation recorded in the potential range (a) from −0.6 to 1.0 V and (b) from −1.6 to 1.3 V; 2 mM, 20 mV s^{-1}, 20 °C.

When the reduction of σ-dimers is excluded by setting the switching potential at 0.0 V (Figure 5b), the corresponding CVs show in successive scans decreasing first (0.45 V) and second oxidation peaks (from 1.2 V) of the primary educt ***p*-TTA** as well as a reduction wave at E_{pc} = 0.24 V in analogy to CVs recorded at −45 °C (Figure 4a). However in this case, the redox wave at E_{pa} = 0.79 V resulting from the reversible oxidation of **MMPC** rises significantly displaying an increasing concentration of carbazole under repeated cycling.

The measurements carried out at RT unambiguously reveal that the reactivity of the system is higher than at lower temperatures and that intramolecular carbazole formation (**MMPC**) prevails over intermolecular coupling processes of charged species. This is in agreement with literature data which clearly show that a decrease in temperature favors the intermolecular dimerization of charged species due to the enlargement of the dielectricity constant and to entropic effects.[31,32,38,44,56] For example, CV experiments on the dimerization of 1,3,5-tripyrrolidonobenzene disclose an increase of the dimerization constant as the temperature decreases.[45]

Polymeric Triphenylamines PSTPA and PoTTA. In our previous work on a **PSTPA** polymer with electroactive nonsubstituted **TPA** units in the side chain (CHART 1a), we could show that the dimerization reaction of **TPA** units takes place also in polymeric compounds (Supporting Information, Figure S7).[19] The coupling to **TPB**-moieties and cross-linking occurred under thin layer conditions almost quantitatively. Here, we have studied the coupling behavior of a **PoTTA** polymer (Chart 1b) containing triphenylamines covalently linked to the polymer backbone and with two methyl blocked reactive para sites. Up to now the literature on *para*-methyl-substituted **TPA** polymers or analogous systems has not discussed any coupling reactions which we attribute to the study of only limited potential ranges.[8,9,57]

Our spectroelectrochemical data on the **PoTTA** polymer resemble the low molecular weight counter parts. The reversible radical cation formation up to potentials of 1 V is clearly visible. The CV in Figure 6a depicts a redox wave of the chemically reversible process with E_{pa} = 0.54 V and E_{pc} = 0.36 V ($E_{1/2}$ = 0.45 V) for **PoTTA**/**PoTTA**$^{\bullet+}$ redox couple. The CV in Figure 6b exhibits the products of follow-up reactions applying a higher switching potential of 1.3 V. New redox waves at E_{pa} = 0.96 V and E_{pc} = 0.82 V with $E_{1/2}$ = 0.89 V as well as new broad cathodic waves at −0.42 and −1.03 V are detected.

The oxidation behavior of the polymer **PoTTA** is even more complicated than that of the low molecular compound ***p*-TTA**. The $E_{1/2}$ = 0.89 V is attributed to intramolecular carbazole formation. Between 0 and −1.6 V two broad instead of one broad reduction wave are seen. One possible explanation is that several coupling products are possible likely due to higher local concentration of reactive centers in polymer chains.[19] On the other hand, it can mean that σ-dimers in **PoTTA** are more stable. Experiments at lower temperatures show that the irreversibility of σ-dimer formation increases with temperature decrease which is consistent with literature findings: for permethyl-substituted bithiophene the rate constant for the bond cleaving reaction at low temperatures diminished more rapidly than for the dimerization suggesting that the coupling step becomes irreversible.[25] The irreversibility of σ-dimer formation is also supported by spectroscopic results (not shown).

The absorption spectra corresponding to the CV in Figure 6b are available in Figure S8 of the Supporting Information.

These experiments clearly reveal that σ-coupling in conjugated monomers, oligomers, and polymers does not only occur on the level of the monocationic state but may also take place at higher charging levels of the systems. This may be an important point in the understanding of the formation and charging process of conducting polymers.[26,44]

■ CONCLUSION

The spectroelectrochemical study of the oxidation behavior of *para*-methyl-substituted triphenylamine ***p*-TTA** and its polymeric analogon **PoTTA** exhibits a high reactivity in the dicationic charged state which is evidenced by two simultaneous parallel follow-up coupling reactions. (1) By an irreversible intramolecular coupling reaction the formation of carbazole units is induced. (2) A reversible intermolecular coupling reaction results in the formation of σ-dimers. Whereas the generation of carbazole is described in literature, the formation of charged σ-dimers has not been reported so far and is also unexpected since the para sites are blocked by the methyl groups. Our UV/vis and spectroelectrochemistry data prove the existence of the σ-dimers upon charging to the dicationic state. Depending on the temperature either intra- or intermolecular coupling is favored.

Such self-association processes upon doping may play an important role for polymeric components in optoelectronic applications.

dx.doi.org/10.1021/jp208076z |*J. Phys. Chem. B* 2012, 116, 30–39

■ ASSOCIATED CONTENT

Supporting Information. Further experimental data for dimerization mechanism of **TPA**, **PHC**, and **TPB**. Further experimental evidence of coupling products upon oxidation of ***p*-TTA** to higher oxidation potentials. Scan rate dependence of CVs. In situ spectroelectrochemistry at room temperature. Spectroelectrochemistry of polymeric triphenylamines. This information is available free of charge via the Internet at http://pubs.acs.org

■ AUTHOR INFORMATION

Corresponding Author

*E-mail: sabine.ludwigs@ipoc.uni-stuttgart.de (S.L.); juergen.heinze@physchem.uni-freiburg.de (J.H.).

Present Addresses

#IPOC-Functional Polymers, Institut für Polymerchemie, Universität Stuttgart, Pfaffenwaldring 55, 70569 Stuttgart, Germany.

■ ACKNOWLEDGMENT

S.L. acknowledges financial support by the DFG for an Emmy Noether grant and a Junior Fellowship in FRIAS and by the "Landesstiftung Baden Württemberg". O.Y. acknowledges financial support of her academic studies from the Heinrich Böll Stiftung. J.H. acknowledges financial support by the Fonds der Chemischen Industrie. We thank J. Schneider for lab assistance in characterization.

■ REFERENCES

(1) Smie, A.; Heinze, J. *Angew. Chem., Int. Ed.* **1997**, *36*, 363–367.
(2) Thelakkat, M. *Macromol. Mater. Eng.* **2002**, *287*, 442–461.
(3) Stolka, M.; Pai, D. M.; Renfer, D. S.; Yanus, J. Y. *J. Polym. Sci. Polym. Chem. Ed.* **1983**, *21*, 969–983.
(4) Bellmann, E.; Shaheen, S. E.; Thayumanavan, S.; Barlow, S.; Grubbs, R. H.; Marder, S. R.; Kippelen, B.; Peyghambarian, N. *Chem. Mater.* **1998**, *10*, 1668–1676.
(5) Behl, M.; Hattemer, E.; Brehmer, M.; Zentel, R. *Macromol. Chem. Phys.* **2002**, *203*, 503–510.
(6) Kwak, J.; Bae, W. K.; Zorn, M.; Woo, H.; Yoon, H.; Lim, J.; Kang, S. W.; Weber, S.; Butt, H.-J.; Zentel, R; Lee, S.; Char, K.; Lee, C. *Adv. Mater.* **2009**, *21*, 5022–5026.
(7) Snaith, H. J.; Whiting, G. L.; Sun, B.; Greenham, N. C.; Huck, W. T. S.; Friend, R. H. *Nano Lett.* **2005**, *5*, 1653–1657.
(8) Sommer, M.; Lindner, S. M.; Thelakkat, M. *Adv. Funct. Mater.* **2007**, *17*, 1493–1500.
(9) Choi, K.; Yoo, S. J.; Sung, Y.-E.; Zentel, R. *Chem. Mater.* **2006**, *18*, 5823–5825.
(10) Heun, S.; Borsenberger, P. M. *Chem. Phys.* **1995**, *200*, 245–255.
(11) Borsenberger, P. M.; Pautmeier, L.; Richert, R.; Bässler, H. *J. Chem. Phys.* **1991**, *94*, 8276–8281.
(12) Heun, S.; Borsenberger, P. M. *Physica B* **1995**, *216*, 43–52.
(13) Borsenberger, P. M. *J. Appl. Phys.* **1990**, *66*, 5188–5194.
(14) Esposti, A. D.; Fattori, V.; Sabatini, C.; Casalbore-Miceli, G.; Marconi, G. *Phys. Chem. Chem. Phys.* **2005**, *7*, 3738–3743.
(15) Creason, S. C.; Wheeler, J.; Nelson, R. F. *J. Org. Chem.* **1972**, *37*, 4440–4446.
(16) Nelson, R. F.; Philp, R. H. *J. Phys. Chem.* **1979**, *83*, 1979–713.
(17) Seo, E. T.; Nelson, R. F.; Fritsch, J. M.; Marcoux, L. S.; Leedy, D. W.; Adams, R. N. *J. Am. Chem. Soc.* **1966**, *88*, 3498–3503.
(18) Sreenath, K.; Suneesh, C. V.; Kumar, V. K. R.; Gopidas, K. R. *J. Org. Chem.* **2008**, *73*, 3245–3251.
(19) Yurchenko, O.; Heinze, J.; Ludwigs, S. *ChemPhysChem* **2010**, *11*, 1637–1640.
(20) Nelson, R. F.; Adams, R. N. *J. Am. Chem. Soc.* **1968**, *90*, 3925–3930.
(21) Wolf, U.; Bässler, H.; Borsenberger, P. M.; Gruenbaum, W. T. *Chem. Phys.* **1997**, *222*, 259–267.
(22) Jäger, C.; Haarer, D.; Peng, B.; Thelakkat, M. *Appl. Phys. Lett.* **2004**, *85*, 6185–6187.
(23) Bruning, W. H.; Nelson, R. F.; Marcoux, L. S.; Adams, R. N. *J. Phys. Chem.* **1967**, *71*, 3055–3057.
(24) Chiu, K. Y.; Su, T. X.; Li, J. H.; Lin, T.-H.; Liou, G.-S.; Cheng, S.-H. *J. Electroanal. Chem.* **2005**, *575*, 95–101.
(25) Heinze, J.; John, H.; Dietrich, M.; Tschuncky, P. *Synth. Met.* **2001**, *119*, 49–52.
(26) Heinze, J.; Frontana-Uribe, B. A.; Ludwigs, S. *Chem. Rev.* **2010**, *110*, 4724–4771.
(27) Barth, M.; Guilerez, S.; Bidan, G.; Bras, G.; Lapkowski, M. *Electrochim. Acta* **2000**, *45*, 4409–4417.
(28) Bäuerle, P. *Adv. Mater.* **1992**, *4*, 102–107.
(29) Smie, A.; Synowczyk, A.; Heinze, J.; Alle, R.; Tschuncky, P.; Götz, G.; Bäuerle, P. *J. Electroanal. Chem.* **1998**, *452*, 87–95.
(30) Engelmann, G.; Kossmehl, G.; Heinze, J.; Tschuncky, P.; Jugelt, W.; Welzel, H.-P. *J. Chem. Soc., Perkin Trans.* **1998**, *2*, 169–175.
(31) Hill, M. G.; Penneau, J.-F.; Zinger, B.; Mann, K. R.; Miller, L. L. *Chem. Mater.* **1992**, *4*, 1106–1113.
(32) Merz, A.; Kronberger, J.; Dunsch, L.; Neudeck, A.; Petr, A.; Parkanyi, L. *Angew. Chem., Int. Ed.* **1999**, *38*, 1442–1446.
(33) Wakamiya, A.; Nishinaga, T.; Komatsu, K. *Chem. Commun.* **2002**, 1192–1193.
(34) El-Desoky, H.; Heinze, J.; Ghoneim, M. M. *Electrochem. Commun.* **2001**, *3*, 697–702.
(35) Savéant, J.-M. *Acta Chem. Scand. B* **1983**, *37*, 365–378.
(36) Heinze, J.; Rasche, A. *Electrochem. Commun.* **2003**, *5*, 776–781.
(37) Bäuerle, P.; Segelbacher, U.; Maier, A.; Mehring, M. *J. Am. Chem. Soc.* **1993**, *115*, 10217–10223.
(38) Bäuerle, P.; Segelbacher, U.; Gaudl, K.-U.; Huttenlocher, D.; Mehring, M. *Angew. Chem., Int. Ed. Engl.* **1993**, *32*, 76–78.
(39) Levillain, E.; Roncali, J. *J. Am. Chem. Soc.* **1999**, *121*, 8760–8765.
(40) Miller, L. L.; Yu, Y.; Gunic, E.; Duan, R. *Adv. Mater.* **1995**, *7*, 547–548.
(41) Graf, D. D.; Campbell, D. K.; Miller, G. G.; Mann, K. R. *J. Am. Chem. Soc.* **1996**, *118*, 5480–5481.
(42) Smie, A.; Heinze, J. *Angew. Chem.* **1997**, *109*, 375–379.
(43) Tschuncky, P.; Heinze, J.; Smie, A.; Engelmann, G.; Koßmehl, G. *J. Electroanal. Chem.* **1997**, *433*, 223–226.
(44) Heinze, J.; Tschuncky, P.; Smie, A. *J. Solid State Electrochem.* **1998**, *2*, 102–109.
(45) Heinze, J.; Willmann, C.; Bäuerle, P. *Angew. Chem., Int. Ed.* **2001**, *40*, 2861–2864.
(46) Rasche, A.; Heinze, J. *Electrochim. Acta* **2008**, *53*, 3812–3819.
(47) Geskes, C.; Heinze, J. *J. Electroanal. Chem.* **1996**, *418*, 167–173.
(48) Ambrose, J. F.; Carpenter, L. L.; Nelson, R. F. *J. Electrochem. Soc.* **1975**, *122*, 876–894.
(49) Heinze, J.; Hinkelmann, K.; Dietrich, M.; Mortensen, J. *Ber. Bunsen. Phys. Chem.* **1985**, *89*, 1225–1229.
(50) Heinze, J. *NATO ASI Series*, series E, Kluwer Publishers: Dordrecht, 1991; Vol. 197, pp 283−294.
(51) Amthor, S.; Noller, B.; Lambert, C. *Chem. Phys.* **2005**, *316*, 141–152.
(52) Reynolds, R.; Line, L. L.; Nelson, R. F. *J. Am. Chem. Soc.* **1974**, *96*, 1087–1092.
(53) Matis, M.; Rapta, P.; Lukeš, V.; Hartmann, H.; Dunsch, L. *J. Phys. Chem. B* **2010**, *114*, 4451–4460.
(54) Lamm, W.; Pragst, F.; Jugelt, W. *J. Prakt. Chem.* **1975**, *317*, 995–1004.

(55) Hermolin, J.; Levin, M.; Kosower, E. M. *J. Am. Chem. Soc.* **1981**, *103*, 4801–4807.
(56) Graf, D. D.; Duan, R.; Campbell, J. P.; Miller, L. L.; Mann, K. R. *J. Am. Chem. Soc.* **1997**, *119*, 5888–5899.
(57) Bender, T. P.; Graham, J. F.; Duff, J. M. *Chem. Mater.* **2001**, *13*, 4105–4111.